Computers and Concrete, *Vol. 31, No. 6 (2023) 545-559*
https://doi.org/10.12989/cac.2023.31.6.545

An empirical relationship for compressive strength of preplaced aggregate concrete with modified binder

Kunal Krishna Das[1,2], Eddie Siu-Shu Lam[1] and Jeong Gook Jang[2*]

[1]*Department of Civil and Environmental Engineering, The Hong Kong Polytechnic University, Hung Hom, Hong Kong*
[2]*Division of Architecture and Urban Design, Urban Sciences Institute, Incheon National University, 119 Academy-ro, Yeonsu-gu, Incheon 22012, Republic of Korea*

(*Received November 28, 2022, Revised February 8, 2023, Accepted February 13, 2023*)

Abstract. In this study, an experimental investigation was conducted to assess the influence of ground granulated blast furnace slag (GGBS) and silica fume (SF) on the fresh and hardened properties of grout specimens and preplaced aggregate concrete (PAC). Grout proportions were optimized statistically using a factorial design and were applied to 10 mm and 20 mm coarse aggregates to produce PAC. The results demonstrate that GGBS has a more significant effect on the compressive strength of grout compared to SF, with a small increase or decrease in the GGBS content having a greater influence on the compressive strength of grout than SF. The water to binder ratio had the most significant effect on the compressive strength of PAC, followed by the coarse aggregate size and sand to binder ratio. An empirical relationship to predict the compressive strength of PAC was proposed through an experimentally derived factorial design along with a statistical analysis of collectively obtained data and a deep literature review. The results predicted by the empirical relationship were in good agreement with those of PAC produced for verification.

Keywords: compressive strength; empirical relationship; ground granulated blast furnace slag; preplaced aggregate concrete; silica fume

1. Introduction

Preplaced aggregate concrete (PAC) is a type of concrete that is produced in two stages. Firstly, coarse aggregates are placed into a formwork. Secondly, a cementitious grout is injected to fill the voids between the coarse aggregates. PAC is also known as two-staged concrete (Najjar *et al.* 2014), polcrete (Abdelgader 1995) and prepacked concrete (Awal Abdul 1988). Because the coarse aggregates are pre-placed, it can occupy 60% to 70% of the total volume, leaving 30% to 40% of voids between the coarse aggregates to be filled by grout (Najjar *et al.* 2014). A higher coarse aggregate content requires less cement (Stempkowska *et al.* 2020) as compared to conventional concrete. This makes PAC relatively economical, reduces the heat of hydration, and lowers its susceptibility to drying shrinkage (davis 1960, Najjar *et al.* 2014, Tuyan *et al.* 2020a). The mechanical properties of PAC differ from those of conventional concrete. In PAC, the applied stress is transferred through the skeleton of coarse aggregates and then to the hardened grout after deformation (Abdelgader and Górski 2002), unlike in conventional concrete where the applied stress is transferred homogenously throughout the matrix. The type and size of the coarse aggregates, the grout composition, and the properties of the grout all have strong effects on the mechanical properties of PAC.

Voids between the coarse aggregates provide passageways through which the grout can pass. Hence, with a reduction in the size of the coarse aggregate, the voids between the coarse aggregates become narrow and complicate the application of the grout (Das and Lam 2019). While there are no specific limitations on the maximum size of the coarse aggregates to be used, the smallest coarse aggregate size is governed by the desired flowability and penetrability of the grout (Najjar *et al.* 2014). The smallest size of coarse aggregates used is recommended to be at least four times the largest size of the fine aggregate used (Najjar *et al.* 2014, Orchard 1973).

On the other hand, the production of cement alone accounts for the world's third-largest anthropogenic emissions of CO_2 (Tuyan *et al.* 2020b), hence, the use of industrial by-products in the form of supplementary cementitious materials is attractive to reduce the overall carbon footprint while also providing economic benefits. Supplementary cementitious materials such as fly ash have been used extensively to improve the properties of PAC (Bayer 2004, Coo and Pheeraphan 2015, 2016, Najjar 2016, Nehdi *et al.* 2017a, Nowek *et al.* 2007, Vieira *et al.* 2010). A partial replacement of cement with fly ash by up to 33% is recommended in the ACI 304.1 (2005) specification to reduce the heat of hydration. A blend of 10% fly ash and 6% silica fume (SF) as a partial replacement of cement represented the optimum percentages for binder replacement (Nowek *et al.* 2007). The incorporation of SF significantly reduced the flowability of grout (Das *et al.* 2020, Najjar 2016) and is recommended to be used in

*Corresponding author, Professor
E-mail: jangjg@inu.ac.kr

ISSN: 1598-8198 (Print), 1598-818X (Online)

combination with a superplasticizer (Abdelgader and El-Baden 2015). The unfavorable effect of SF on the flowability of grout limits its application to PAC. While studies of the incorporation of ground granulated blast furnace slag (GGBS) (Bayer, 2004) and SF (Abdelgader and El-Baden 2015, Najjar 2016, O'Malley and Abdelgader 2010) in PAC have been conducted, such studies are relatively scarce in comparison to those focusing on conventional concrete. The use of industrial by-products such as GGBS and SF is important not only to reduce the detrimental impact on the environment and lower the cost of production but also to improve the properties of PAC. For instance, in conventional concrete, partial replacement of cement by GGBS by up to 50% is recommended to achieve sulfate resistance and a low-temperature rise in warm temperatures. Partial replacement of cement by GGBS by not more than 20% to 30% is recommended to achieve early strength for an earlier release of the formwork or for application to thin sections at low temperatures (ACI 233R 1995). At ages of 28 days to 90 days and beyond, the presence of GGBS in concrete was found to be highly beneficial at 40% to 60% replacement rates with strength exceeding that of mixes without GGBS. However, a noticeable strength reduction at all ages was observed at 80% replacement of cement by GGBS (Khatib and Hibbert 2005). Further, concretes produced using slag cement displayed substantially lower chloride ion permeability compared to that of other types of cement such as sulfate-resisting cement or Portland cement blended with fly ash (Yildirim *et al.* 2011). The partial replacement of cement by SF in conventional concrete enhances the early strength with no detrimental effect on the long-term strength. This greatly improves the resistance to the transport of water and diffusion of harmful ions, exhibiting superior resistance to chloride ion penetration (Poon *et al.* 2006). Increasing the SF content increases the compressive strength of concrete. A blend of Portland fly ash and SF displayed high compressive strength, attributed to both the filler effect and the pozzolanic reaction of the SF, giving the cement matrix a denser microstructure and thereby resulting in a significant strength gain (Nochaiya *et al.* 2010).

Many codes of practice and standards provide the basis for the mix designs of conventional concrete with desired properties (ACI 211.1 1996, BS EN 8500 2002, IS 10262 2009). They offer recommendations to produce concrete to specified strength and workability levels, avoiding excessive trial mixes and reducing resource waste. As the casting technique of PAC differs from that of conventional concrete, the mix design of conventional concrete is not suitable for PAC. Empirical relationships have been proposed for estimations of the tensile strength using the compressive strength of PAC (Abdelgader and Ben-Zeitun 2005, Abdelgader and Elgalhud 2008, Abdelgader and Górski 2003, Najjar *et al.* 2014, Rajabi *et al.* 2020, Rajabi and Omidi Moaf 2017). The empirical relationships between the water to binder ratio, the sand to binder ratio, and the compressive strength of PAC have also been proposed (Abdelgader and Elgalhud 2008). However, the coarse aggregate size and grout constituents along with the binder composition and proportion are significant parameters affecting the compressive strength of PAC. Thus, these factors require consideration.

In this study, the partial replacement of cement was applied while varying the GGBS and SF levels from 0 to 40% and from 0 to 10% by weight of the binder, respectively. A factorial design was used to optimize the grout proportions. Various grout proportions were then selected to produce and investigate the properties of PAC. An empirical relationship was proposed to predict the 28-day compressive strengths of PAC from the constituent components of the grout and the coarse aggregate size. A binder factor, developed through an experimental investigation and a statistical analysis, was linked to the empirical relationship to account for the change in the compressive strength of PAC due to the incorporation of GGBS and/or SF.

2. Experimental program

An experimental investigation was conducted to evaluate the effects of GGBS and SF on the grouts and PAC. Grout proportions were optimized statistically using a factorial design. PAC was formed using different sizes of coarse aggregates. The flowability and compressive strength of the grout were assessed. The mechanical properties of the PAC, in this case the compressive strength and the splitting tensile strength, were accessed. The durability of the PAC was evaluated in terms of chloride ion penetration and drying shrinkage.

Mix proportions along with the 28-day compressive strengths of the PAC were obtained from a deep literature review and were statistically analyzed to determine the empirical relationships between the coarse aggregate size, the water to binder ratio, the sand to binder ratio, and the compressive strength of the PAC. A binder factor Beta was developed from the above-mentioned experimental investigation and statistical analysis and then incorporated into the empirical relationship to account for the change in the compressive strength due to the incorporation of GGBS and/or SF. Further, PAC mixes were produced to verify and determine the predictive ability of the developed empirical relationships.

2.1 Materials

Ordinary Portland cement of type I conforming to ASTM C 150 (2017) was used. GGBS and SF were sourced locally in Hong Kong. SF was received in dry densified form. The chemical compositions of the cement, GGBS, and SF, as analyzed by X-ray fluorescence, are shown in Table 1. The particle size distributions of the cement, GGBS, and SF are shown in Fig. 1. The ultimate particle size of SF is well known to be exceedingly small (Diamond and Sahu 2006) which was in contrast to the observed particle size distribution in Fig.1. In general, the diameters of SF particles might correspond to the diameters of the individual spheres (if the spheres are disconnected from each other) which reflects the small size. However, the dispersibility of SF into an assembly of isolated spheres

Table 1 Chemical composition of cement, GGBS, and SF

Material	MgO	Al_2O_3	SiO_2	P_2O_5	SO_3	K_2O	CaO	TiO_2	MnO	Fe_2O_3
Cement	0.95	5.25	20.48	-	1.90	0.40	65.00	-	-	3.82
GGBS	6.88	16.90	31.70	0.09	2.45	0.51	40.10	0.80	0.28	0.27
SF	2.25	0.48	90.30	0.19	0.61	2.94	0.99	-	0.14	1.24

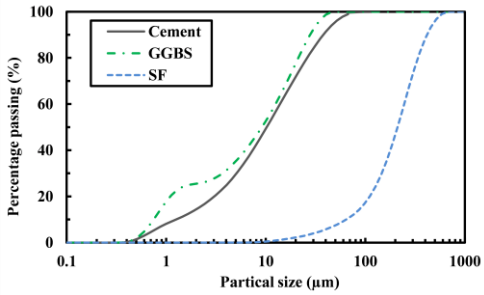

Fig. 1 Particle size distribution of cement, GGBS, and SF

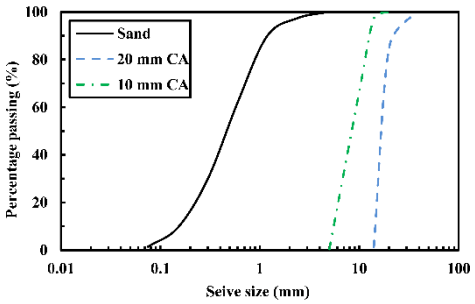

Fig. 2 Particle size distribution of sand, 10 mm coarse aggregates (10 mm CA) and 20 mm coarse aggregates (20 mm CA)

may not be possible due to fused links existing between them at the points of contact, leading to the sintering of dozens or hundreds of linked spheres into clusters (Diamond and Sahu 2006, Krakowiak *et al.* 2018, St. John 1994). Further in this study, the particle size distribution of binder was determined by laser diffraction particle size analyser (LS13 320) and most of the laser diffraction particle size analyzers record the smallest size in the range of clusters rather than in the fine sizes of individual spheres. A similar observation was reported by Diamond and Sahu (2006), where significant proportions of various densified fumes measured in the range of 10 μm to100 μm with some of the fumes displaying significant contents of particles between 100 μm and 1000 μm. This was ascribed to the presence of intertwined chains of linked particles within agglomerates, largely responsible for the stability of most of the agglomerates against dispersion (St. John 1994).

A polycarboxylate-type polymer-based superplasticizer (ADVA 109) was employed to obtain the desired flowability of the grouts. River sand with specific gravity of 2.65, conforming to Grade 3, ACI 304.1 (2005), was used as fine aggregates. The sand was readily available in the laboratory and falls within the recommended ACI limits. Further, the presence of a lower coarser fraction in sand prevents the possibility of clogging the voids in between the coarse aggregates during grouting. Crushed granites of siliceous mineralogy, sized 10 mm and 20 mm, were used as coarse aggregates. The maximum coarse aggregate size was limited to less than a quarter of the diameter of the cylindrical molds used. The coarse aggregates and sand gradation is shown in Fig. 2. The measured void contents of the 10 mm and 20 mm coarse aggregates were 28.55% and 37.63%, respectively. The void content refers to the space between the coarse aggregate skeleton to be occupied by grout.

For the preparation of specimens, moulds were cleaned and applied with a thin film of oil. The moulds were then filled with coarse aggregates of the required size. The top surface of the moulds was levelled gently with a metal rod.

To prepare the grouts, the dry ingredients, i.e., cement, supplementary cementitious materials, and sand were first mixed in the mixer for 5 minutes. SP mixed with water was then added steadily to the dry mix. Mixing was continued for another 2 to 3 minutes to ensure the consistency of the grout. Once the grout was prepared, it was gently poured into the moulds and was allowed to penetrate through the coarse aggregates under the action of gravity. The specimens were demoulded in 24 hours and cured under water for 28 days.

2.2 Specimens and tests

Bleeding tests on the grouts were conducted as per ASTM C 940 (2016), and the bleeding of all grout mixes was within the permissible limits, i.e., bleeding of less than 2% after 120 minutes. Grout consistency was determined by flow cone tests conforming to ASTM C 939 (2002). A grout compression test at 28 days was performed as per ASTM C 942 (2008) using cubes with 50 mm sides. PAC was produced using the gravity process, where the grout was poured onto the surface of coarse aggregates and was allowed to flow under the action of gravity. Compressive strength and splitting tensile strength tests of the PAC were performed using 100 mm×200 mm (diameter×length) cylinders in accordance with ASTM C 39 (2005) and ASTM C 496 (2011), respectively. Cylinders with 100 mm diameters were cut into 50 mm thick slices to determine the chloride ion penetration according to ASTM C 1202 (2012) at 28 days. 75 mm×75 mm×285 mm prisms were prepared to determine the drying shrinkage of PAC as per BS ISO 1920-8 (2009) and were tested during a period of 90 days.

2.3 Design of the experiment for the grout mix proportions

The parameters in the experiment were considered by applying a two-level full factorial design (2^k) to the grout, where 2 denotes the level of each factor and the superscript

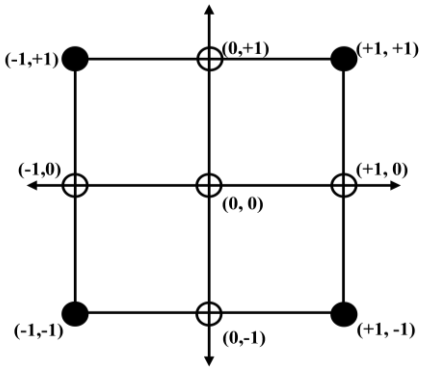

Fig. 3 Face-centered central composite design

Table 2 Coded levels and actual ratios of GGBS and SF in grout

Sl. no.	Mix ID	Coded level		Actual material ratio	
		GGBS/B	SF/B	GGBS/B	SF/B
1	GRT0000	-1	-1	0.00	0.00
2	GRT4005	1	0	0.40	0.05
3	GRT0010	-1	1	0.00	0.10
4	GRT2010	0	1	0.20	0.10
5	GRT2005	0	0	0.20	0.05
6	GRT4010	1	1	0.40	0.10
7	GRT2005	0	0	0.20	0.05
8	GRT2000	0	-1	0.20	0.00
9	GRT0005	-1	0	0.00	0.05
10	GRT4000	1	-1	0.40	0.00
11	GRT2005	0	0	0.20	0.05

Table 3 Mix proportion of PAC

Sl. no.	Mix ID	Coarse aggregate size (mm)	GGBS/B	SF/B
1	PAC0000-20	20	0.00	0.00
2	PAC4000-20	20	0.40	0.00
3	PAC0010-20	20	0.00	0.10
4	PAC2005-20	20	0.20	0.05
5	PAC4010-20	20	0.40	0.10
6	PAC0000-10	10	0.00	0.00
7	PAC4000-10	10	0.40	0.00
8	PAC0010-10	10	0.00	0.10
9	PAC2005-10	10	0.20	0.05
10	PAC4010-10	10	0.40	0.10

k is the number of factors to be studied (Montgomery D.C. 2017). Two factors were selected: GGBS/B and SF/B. Center points were included, forming a face-centered central composite design (shown in Fig. 3). To estimate the experimental errors, the center point (later referred to as GTR2005) was replicated twice. To remove all sources of extraneous variation, the mixes were prepared in a random order (Coo and Pheeraphan 2015). Levels for the high, midpoint, and low values were +1, 0, and -1, respectively. A linear regression analysis was used to analyze the data.

2.4 Mix design of grout and PAC

Based on the trial mixes, the water to binder ratio (W/B) was assigned the lowest possible value of 0.33. The superplasticizer (SP) dosage was modified to obtain an efflux time of less than 20 seconds. The maximum SP dosage was limited to 1.5% by weight of the binder to prevent excess bleeding of the grout. As sand can significantly reduce the flowability of grout (Abdelgader 1996, Abdelgader *et al.* 2013, Coo and Pheeraphan 2015), the sand to binder ratio (S/B) was set to zero. This may isolate the effects of GGBS and SF on the grout while also achieving a suitable efflux time. Hence, the W/B and S/B ratios for all mixes were set constant at 0.33 and 0.00, respectively.

GGBS and SF were used to replace cement partially at 0 to 40% and 0 to 10% by weight of the binder, respectively. The ratios for GGBS and SF were optimized by evaluating the efflux time and compressive strength of the grout. Samples were prepared by trial and error to determine the GGBS/B and SF/B ratios. The compressive strength of the grout decreased significantly (by more than 30%) with partial cement replacement by GGBS above 40%. Therefore, partial replacement with GGBS was limited to 40%. The flowability of the grout decreased significantly when the partial replacement of cement by SF exceeded 10%. With 10% SF as a partial replacement of cement, the maximum SP dosage was applied to achieve an efflux time of less than 20 seconds. Hence, partial replacement of cement by SF was limited to 10%. Table 2 shows the proportions of GGBS and SF in the grout. The lowest factor levels (-1) for both GGBS/B and SF/B were set to 0.00, representing a pure cement-water grout. The highest factor levels (+1) for GGBS/B and SF/B were set to 0.40 and 0.10, respectively. As to the mix IDs (e.g., GRT0000), GRT represents grout, whereas the first two digits represent the mix proportion of GGBS and the following two digits depict the mix proportion of SF. An average of three specimens were considered for determining the 28 days compressive strength.

Selected grout mixes with the highest and lowest factor levels (i.e., +1 and -1) and midpoint factor level (i.e., 0) were used to produce PAC. As it is recommended that the minimum size of coarse aggregates be at least four times larger than that of the maximum size of the fine aggregates used in grout (Najjar *et al.* 2014, Orchard 1973), the elimination of sand from the grout enabled a significant reduction in the coarse aggregate size. Hence, 10 mm and 20 mm coarse aggregates were employed to produce the PAC here. The mix design of the PAC is shown in Table 3. Regarding the mix IDs (e.g., PAC0000-20), PAC is followed by the proportions of GGBS and SF in the grout. The first two digits represent the binder proportion of GGBS and the last two digits represent the binder proportion of SF. The coarse aggregate size follows the

Table 4 28 days compressive strength of grout and binder factor β

Sl. no.	Mix ID	Superplasticizer at the rate of binder (%)	Efflux time (sec)	28 days compressive strength (MPa)	Standard deviation (MPa)	β
1	GRT0000	1.00	19.22	87.05	0.93	1.00
2	GRT4005	0.84	19.16	74.08	1.34	0.85
3	GRT0010	1.50	19.19	93.00	1.86	1.07
4	GRT2010	1.20	20.69	83.89	1.48	0.96
5	GRT2005	1.00	18.89	79.83	0.92	0.92
6	GRT4010	1.24	20.37	80.21	1.04	0.92
7	GRT2005	1.00	18.18	80.10	0.27	0.92
8	GRT2000	0.70	21.00	75.12	2.88	0.86
9	GRT0005	1.15	17.53	89.32	1.13	1.03
10	GRT4000	0.60	16.03	68.85	1.73	0.79
11	GRT2005	1.00	18.97	80.97	0.73	0.93

β is a relative value with reference to GRT0000 and is elaborated in Section 4.2.

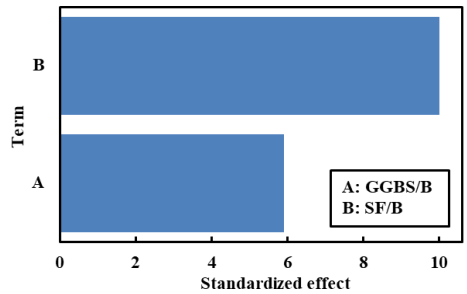

Fig. 4 Pareto chart of standardized effects on SP dosage

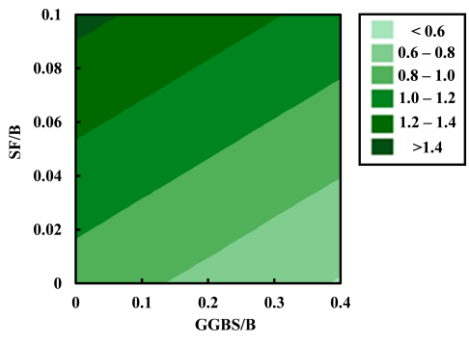

Fig. 5 Contour plot of SP dosage (%) versus SF/B, GGBS/B

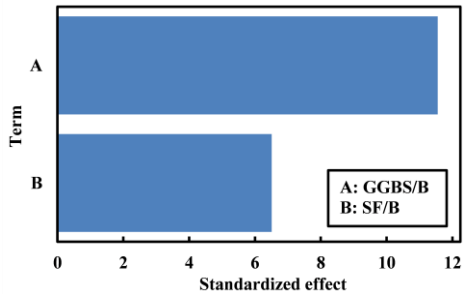

Fig. 6 Pareto chart of standardized effects on grout compressive strength

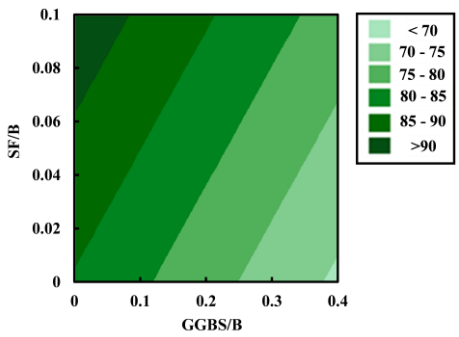

Fig. 7 Contour plot of compressive strength (MPa) versus SF/B, GGBS/B

binder proportions.

3. Results and discussion

3.1 Grout properties

Table 4 shows the efflux time and compressive strength of the grout. The statistical software "Minitab" was used to analyze the data and to plot a Pareto chart and a contour plot. A Pareto chart provides the standardized effects of factors which are represented by bars in descending order. The length of each bar represents the significance of the factor. Figs. 4 and 5 present the Pareto chart and the contour plot of the SP dosage applied to obtain an efflux time of less than 20 seconds, respectively. As shown in Fig. 4, SF/B has a greater effect on the efflux time than GGBS/B. This indicates that a small increase or decrease in the SF content has a larger effect on the flowability of the grout than GGBS. Fig. 5 shows that with an increase of GGBS/B, the SP dosage requirement to achieve an efflux time of less than 20 seconds decreases. This increase in the flowability of the grout due to the incorporation of GGBS can be attributed to the better particle dispersion and the smooth and dense surface characteristics of the GGBS particles, which absorb less water during mixing (Johari *et al.* 2011). With an increase in SF/B, the SP dosage requirement increased, ascribed to an increase in the water demand level

due to the fine particle size of the SF, which decreased the flowability of the grout. At SF/B=0.10, a high dosage of SP (>1.4) was required to maintain an efflux time within 20 seconds. However, the pattern of the contour plot suggests that SF/B can be optimized with GGBS/B to achieve suitable flowability without increasing the SP dosage.

Fig. 6 and Fig. 7 correspondingly show a Pareto chart and contour plot of the compressive strength of the grout at 28 days. GGBS/B has more of an effect on the compressive strength of grout than SF/B. The contour plot shows that high compressive strength was achieved with high levels of SF/B and low levels of GGBS/B. Mixes incorporating the highest level of SF/B with GGBS/B=0 displayed compressive strength above 90 MPa, whereas mixes incorporating the highest level of GGBS/B with SF/B=0 displayed compressive strength below 70 MPa. An increase in the pozzolanic reaction between SiO_2 in SF and $Ca(OH)_2$ from the hydration products results in an increase in the compressive strength brought on by the inclusion of SF (Najjar 2016). The reduction in the compressive strength of the grout due to the inclusion of GGBS was ascribed to the longer period required for the formation of calcium hydroxide (Oner and Akyuz 2007) and the reduction in the cement content caused by the high replacement levels of GGBS.

3.2 PAC properties

3.2.1 Mechanical properties

The compressive strength and splitting tensile strength of the PAC at 28 days are shown in Figs. 8 and 9, respectively. SF improves both the compressive strength and the splitting tensile strength of PAC. This was attributed to the enhanced bonding between the binder and the coarse aggregates, achieved by the elimination of weak linkages between the paste and coarse aggregates at the interfacial transition zone, creating a homogeneous and dense microstructure (Khan & Siddique, 2011). The compressive strength and splitting tensile strength of PAC decrease with the incorporation of GGBS. PAC with 40% GGBS displayed low compressive strength and splitting tensile strength with both 10 mm and 20 mm coarse aggregates. The reduced strength is attributable to the latent reactivity of GGBS and the high dilution levels owing to the substantial replacement of cement with GGBS (Johari *et al.* 2011). The PAC incorporating GGBS exhibited increased strength when optimized with SF. PAC with 40% GGBS and 10% SF displayed strength equivalent to that of PAC without GGBS and/or SF.

With a reduction in the coarse aggregate size from 20 mm to 10 mm, the compressive strength and splitting tensile strength of PAC increased. This likely stems from an increase in the bonding area between the coarse aggregates and the grout and an increase in the mechanical interlocking between the coarse aggregates that improved the frictional properties.

3.2.2 Durability

Fig. 10 shows the chloride ion penetration of PAC. GGBS and SF improve the resistance to chloride ion penetration. PAC produced using 40% GGBS and 10% SF exhibited superior resistance to chloride ion penetration. This is likely due to the high replacement of cement by GGBS and SF. GGBS reduces the porosity of concrete by introducing extra C-S-H gel into the paste and forming a denser microstructure, thereby improving the pore structure (Cheng *et al.* 2005). SF densifies the mix by acting as micro-fillers and improves the microstructure by accelerating the rate of hydration, thereby enhancing the packing density and thus improving the resistance to chloride ion penetration (Poon *et al.* 2006).

A reduction in the coarse aggregate size from 20 mm to 10 mm led to a significant increase in the resistance to chloride ion penetration. With the reduction in the coarse aggregate size, the void content of PAC was reduced (as discussed in section 2.1), reducing the amount of grout per surface area of the PAC. This reduces the passages through which chloride ions can pass and subsequently reduces

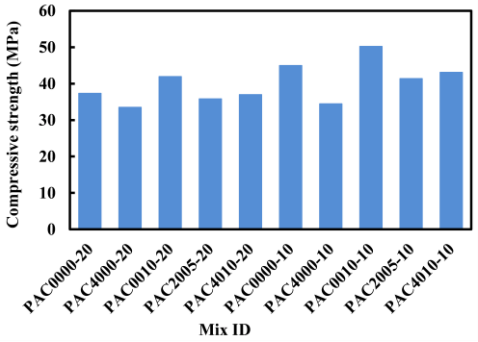

Fig. 8 Compressive strength of PAC

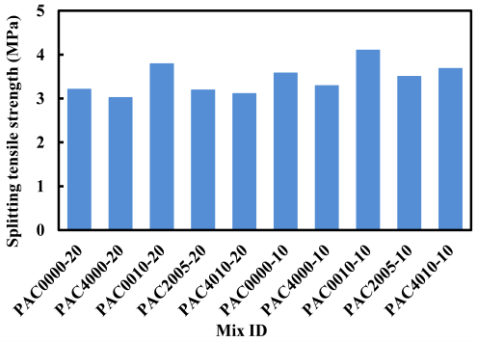

Fig. 9 Splitting tensile strength of PAC

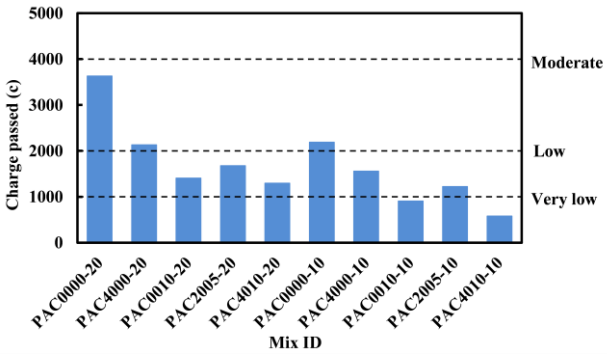

Fig. 10 Chloride ion penetration of PAC

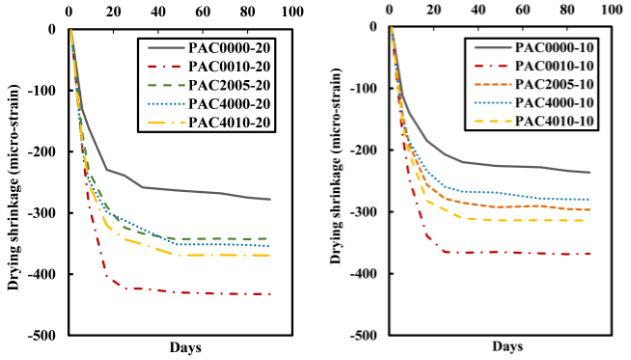

(a) 20 mm CA (b) 10 mm CA

Fig. 11 Drying shrinkage of PAC

chloride ion penetration. Further, due to the weaker restraining effects, the possibility of microcracking in the interfacial transitional zone for concrete produced using smaller-sized coarse aggregates is reduced (Bisschop and Van Mier 2002). This could be another reason for the improved resistance to chloride ion penetration with a decrease in the coarse aggregate size.

Fig. 11 shows the drying shrinkage of PAC. The drying shrinkage of PAC increases with the incorporation of GGBS and SF. GGBS produces a denser mix with fine capillary pores, which increases the capillary pore water pressure, resulting in increased shrinkage strain levels (Saluja *et al.* 2019). The high pozzolanic reaction and pore size refinement mechanism of SF increase the shrinkage of concrete (Rao 2001). SF produces a large amount of C-S-H, which holds a large amount of gel water. The expulsion of this gel water during the drying step increases the shrinkage (Varghese *et al.* 2017).

The drying shrinkage of PAC decreased with the reduction in the coarse aggregate size. This could be attributed to the decreased void content with a decrease in the coarse aggregate size, which subsequently reduces the amount of grout required to produce PAC. Unlike grout paste, coarse aggregates are not apt to shrink due to their low permeability, restricting the overall deformation. Neville (2011) indicated that with a higher aggregate/cement ratio, lower shrinkage strain could be achieved as the fraction of composite material prone to shrinkage decreases. Although the drying shrinkage of PAC increased with the inclusion of GGBS and/or SF, it could still be classified as low-shrinkage concrete (Emmons 1992) and satisfactory resistance to cracking (Fu *et al.* 2016) could still be ensured.

4. Proposed empirical relationship

4.1 Review

The mix proportions of PAC constituting cement-sand grout, compiled from the available literature, were used to develop an empirical relationship to predict the compressive strength of PAC at 28 days. S/B and W/B ratios being the basic constituents of grout were considered as determining parameters of the compressive strength of PAC. The size of coarse aggregates being the primary factor influencing the penetrability of grout through the coarse aggregate skeleton was considered when formulating the compressive strength of PAC. Table 5 shows the mix proportions of the grout and the coarse aggregate sizes used by other authors to produce PAC. As a coarse aggregate size of 20 mm was found to be the optimum size of coarse aggregates to produce PAC using traditional cement-sand grout (Das and Lam 2019), the coarse aggregate size was expressed as the ratio between the maximum nominal size of the coarse aggregates (CA) and 20 mm. While some authors used cylinders to determine the compressive strength of PAC, some used cubes. For consistency, the cube compressive strength was converted into the cylinder compressive strength via multiplication by a factor of 0.8 (BS EN 12504-1 2009). Mix proportions not recommended by other authors or those involving supplementary cementitious materials (Abdelgader and El-Baden 2015 Rajabi *et al.* 2020), fibers (Mohammadhosseini *et al.* 2020, Nehdi *et al.* 2017b, Prasad and Murali 2021), and activators (Lv *et al.* 2020, Siddique *et al.* 2021) were not considered. For the mix proportions considered in Table 5, the penetrability of grout through the preplaced aggregates was considered to be satisfactory. Some of the mix proportions by Abdelgader and Elgalhud (2008) displaying high efflux times (around 80 to 180 seconds) were not considered, as such high efflux times may impede the penetrability of grout through preplaced coarse aggregates and compromise the strength of the PAC. A study conducted by Abdelgader *et al.* (2010) was not considered, as the PAC in their case was designed for underwater applications.

Linear regression was used to analyze the data and determine the effect of the above-mentioned factors on the compressive strength of PAC. Fig. 12 shows a Pareto chart of the compressive strength of PAC. As shown in the figure, W/B had the strongest effect on the compressive strength of PAC, followed by CA. S/B had the shortest bar length, indicating that it had less of an influence on the compressive strength of PAC as compared to W/B and CA. Eq. (1) expresses the empirical relationship between the compressive strength of PAC, CA, W/B, and S/B, suggesting that with the increase in the CA and W/B ratios, the compressive strength of PAC decreases. However, with the increase in the S/B ratio, the compressive strength of PAC increases slightly. Generally, with an increase in the coarse aggregate size, the compressive strength decreases (Alexander and Wardlaw 1960, Bloem and Gaynor 1963, Tumidajski and Gong 2006). Failure of concrete typically occurs at the matrix-coarse aggregate interface. The stresses that develop at the interface, leading to failure, are reduced by increasing the surface area of the coarse aggregates, which is achieved by reducing the coarse aggregate size (Cordon and Gillespie 1963, Rashid and Mansur 2009). The use of small-size coarse aggregates is favorable for improving the structure of the interfacial transition zone (Guo *et al.* 2020). Further, ACI 363 (1997) suggests minimizing the maximum size of coarse aggregates to produce concrete with high compressive strength. Abdelgader (1996) and Abdelgader and Elgalhud (2008)

Table 5 Mix proportions and compressive strength of PAC from previous studies

References	Sl. No.	CA (mm)	CA/20	W/B	S/B	PAC compressive strength (MPa)	PAC cylinder Strength (MPa)	Predicted PAC cylinder strength (MPa)
Lv *et al.* (2020)*	1	9.50	0.48	0.30	1.00	72.00	57.60	46.38
	2	9.50	0.48	0.30	1.50	66.00	52.80	47.56
	3	9.50	0.48	0.30	2.00	57.50	46.00	48.74
	4	9.50	0.48	0.35	1.00	67.50	54.00	43.42
	5	9.50	0.48	0.35	1.50	61.00	48.80	44.59
	6	9.50	0.48	0.35	2.00	52.50	42.00	45.77
	7	9.50	0.48	0.40	1.00	58.00	46.40	40.45
	8	9.50	0.48	0.40	1.50	55.00	44.00	41.62
	9	9.50	0.48	0.40	2.00	45.00	36.00	42.80
	10	9.50	0.48	0.45	1.00	47.50	38.00	37.48
	11	9.50	0.48	0.45	1.50	44.00	35.20	38.66
Cheng *et al.*(2019)*	12	20.00	1.00	0.42	1.00	39.60	31.68	36.62
	13	20.00	1.00	0.42	1.00	43.90	35.12	36.62
	14	20.00	1.00	0.48	1.30	36.20	28.96	33.76
	15	20.00	1.00	0.54	1.60	33.50	26.80	30.91
	16	20.00	1.00	0.42	1.10	48.00	38.40	36.85
	17	20.00	1.00	0.48	1.30	40.00	32.00	33.76
	18	20.00	1.00	0.54	1.60	35.00	28.00	30.91
Das and Lam (2019)	19	45.00	2.25	0.37	0.50	32.20	32.20	32.12
	20	37.00	1.85	0.37	0.50	33.67	33.67	34.13
	21	20.00	1.00	0.37	0.50	42.46	42.46	38.41
	22	45.00	2.25	0.37	0.50	34.65	34.65	32.12
	23	37.00	1.85	0.37	0.50	34.96	34.96	34.13
	24	20.00	1.00	0.37	0.50	43.58	43.58	38.41
Abdelgader *et al.* (2018)*	25	50.00	2.50	0.45	1.50	30.82	24.66	28.47
	26	50.00	2.50	0.50	1.50	27.82	22.26	25.50
	27	50.00	2.50	0.55	1.50	23.72	18.98	22.53
	28	50.00	2.50	0.45	1.00	30.65	24.52	27.29
	29	50.00	2.50	0.50	1.00	27.10	21.68	24.32
	30	50.00	2.50	0.55	1.00	23.55	18.84	21.35
	31	50.00	2.50	0.45	0.80	30.78	24.62	26.82
	32	50.00	2.50	0.50	0.80	27.23	21.78	23.85
	33	50.00	2.50	0.55	0.80	23.68	18.94	20.88
Nehdi *et al.* (2017a)	34	40.00	2.00	0.45	1.00	31.50	31.50	29.80
Mohammadhosseini *et al.* (2016)	35	20.00	1.90	0.50	1.50	33.00	33.00	33.05
	36	20.00	1.90	0.50	1.50	32.00	32.00	33.05
Najjar *et al.* (2016)	37	40.00	2.00	0.44	1.00	31.50	31.50	30.40
Coo and Pheeraphan (2015)*	38	9.50	0.48	0.33	0.00	50.92	40.74	42.25
	39	9.50	0.48	0.33	1.00	57.63	46.10	44.60
	40	25.00	1.25	0.33	0.00	40.37	32.30	38.35
	41	19.00	0.95	0.33	0.50	55.63	44.50	41.04
Saud *et al.* (2014)	42	50.00	2.50	0.45	1.00	32.00	32.00	27.29
	43	50.00	2.50	0.50	1.00	30.00	30.00	24.32
	44	50.00	2.50	0.55	1.00	25.00	25.00	21.35
	45	50.00	2.50	0.65	1.00	17.50	17.50	15.41

Table 5 Continued

References	Sl. No.	CA (mm)	CA/20	W/B	S/B	PAC compressive strength (MPa)	PAC cylinder Strength (MPa)	Predicted PAC cylinder strength (MPa)
Abdelgader *et al.* (2013)*	46	37.40	1.87	0.55	1.00	26.23	20.98	24.52
	47	37.40	1.87	0.65	1.00	16.89	13.51	18.58
	48	37.40	1.87	0.75	1.00	17.56	14.05	12.65
	49	37.40	1.87	0.80	1.00	14.89	11.91	9.68
	50	37.40	1.87	0.65	1.25	20.89	16.71	19.17
	51	37.40	1.87	0.75	1.25	19.78	15.82	13.24
	52	37.40	1.87	0.80	1.25	13.78	11.02	10.27
	53	37.40	1.87	0.65	1.50	24.00	19.20	19.76
	54	37.40	1.87	0.75	1.50	19.78	15.82	13.83
	55	37.40	1.87	0.80	1.50	12.44	9.95	10.86
	56	37.40	1.87	0.65	2.00	24.67	19.74	20.94
	57	37.40	1.87	0.75	2.00	16.89	13.51	15.00
	58	37.40	1.87	0.80	2.00	18.00	14.40	12.03
Abdelgader and Elgalhud (2008)	59	25.00	1.25	0.80	0.50	13.69	13.69	11.62
	60	25.00	1.25	0.80	1.00	15.07	15.07	12.80
	61	25.00	1.25	0.80	1.50	16.01	16.01	13.98
	62	25.00	1.25	0.80	0.50	14.39	14.39	11.62
	63	25.00	1.25	0.80	1.00	15.79	15.79	12.80
	64	25.00	1.25	0.80	1.50	16.31	16.31	13.98
Abdelgader (1999)*	65	63.00	3.15	0.45	1.50	30.36	24.29	25.20
	66	63.00	3.15	0.50	1.50	26.60	21.28	22.23
	67	63.00	3.15	0.55	1.50	22.84	18.27	19.26
	68	63.00	3.15	0.45	1.00	30.34	24.27	24.02
	69	63.00	3.15	0.50	1.00	26.58	21.26	21.05
	70	63.00	3.15	0.55	1.00	22.82	18.26	18.08
	71	63.00	3.15	0.45	0.80	30.33	24.26	23.55
	72	63.00	3.15	0.50	0.80	26.57	21.26	20.58
	73	63.00	3.15	0.55	0.80	22.80	18.24	17.61
	74	63.00	3.15	0.45	1.50	30.82	24.66	25.20
	75	63.00	3.15	0.50	1.50	27.27	21.82	22.23
	76	63.00	3.15	0.55	1.50	23.72	18.98	19.26
	77	63.00	3.15	0.45	1.00	30.65	24.52	24.02
	78	63.00	3.15	0.50	1.00	27.10	21.68	21.05
	79	63.00	3.15	0.55	1.00	23.55	18.84	18.08
	80	63.00	3.15	0.45	0.80	30.78	24.62	23.55
	81	63.00	3.15	0.50	0.80	27.23	21.78	20.58
	82	63.00	3.15	0.55	0.80	23.68	18.94	17.61
	83	63.00	3.15	0.45	1.50	31.05	24.84	25.20
	84	63.00	3.15	0.50	1.50	27.28	21.82	22.23
	85	63.00	3.15	0.55	1.50	23.52	18.82	19.26
	86	63.00	3.15	0.45	1.00	31.14	24.91	24.02
	87	63.00	3.15	0.50	1.00	27.37	21.90	21.05
	88	63.00	3.15	0.55	1.00	23.60	18.88	18.08
	89	63.00	3.15	0.45	0.80	31.20	24.96	23.55
	90	63.00	3.15	0.50	0.80	27.44	21.95	20.58
	91	63.00	3.15	0.55	0.80	23.67	18.94	17.61

Table 5 Continued

References	Sl. No.	CA (mm)	CA/20	W/B	S/B	PAC compressive strength (MPa)	PAC cylinder Strength (MPa)	Predicted PAC cylinder strength (MPa)
Awal Abdul (1988)	92	38.00	1.90	0.52	1.50	28.90	28.90	27.33
	93	38.00	1.90	0.50	1.50	29.00	29.00	28.52

*Indicates that cube strengths were converted to cylinder strengths

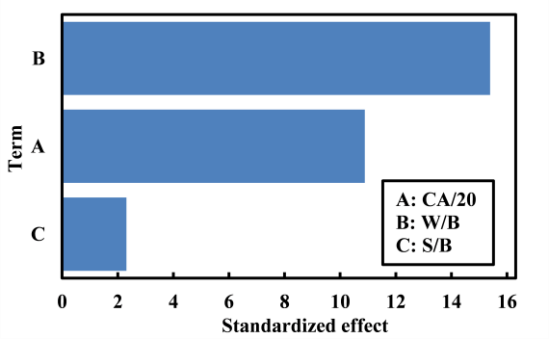

Fig. 12 Pareto chart of standardized effects on compressive strength of PAC

observed that the mechanical properties of PAC were not affected by the amount of sand. Coo and Pheeraphan (2015) suggested that variations of the S/B ratio did not have a significant impact on the mechanical properties of PAC at high W/B ratios (0.4 to 0.6). This was attributed to a weak grout matrix due to excessive free water that leads to bleeding, resulting in the formation of capillary voids in the interface and underneath the coarse aggregates. However, the effects of variations in the amount of sand were observed to be distinct at low W/B ratios (Coo and Pheeraphan 2015), stemming from the high amount of energy required to overcome the resistance to crack propagation and crack growth due to the larger and more angular shapes of sand particles.

$$f_c' = 64.23 - 5.03\left(\frac{CA}{20}\right) - 59.37\left(\frac{W}{B}\right) + 2.35\left(\frac{S}{B}\right) \quad (1)$$

Table 6 shows the model summary of Eq. (1). Sigma (σ) is the standard deviation of the distance between the data values and the fitted values. It is measured in units of the response (MPa in this case) and represents how far the actual values fall from the fitted values. R^2 is the percentage of variation as explained by the equation. It is 1 minus the ratio of the error sum of squares to the total sum of squares. The higher the value of R^2 is, the better the equation fits the data. Adjusted R^2 indicates the significance of the considered factors. It is 1 minus ratio of the mean square error to the mean square total. The lower the difference between R^2 and adjusted R^2 is, the greater the significance of the factors becomes. Predicted R^2 determines how well the equation predicts the data. Equations with larger predicted R^2 values indicate better predictive ability. Based on the model summary, the regression equation developed was considered to have a satisfactory degree of fit. Fig. 13 compares the predicted compressive strength against the actual compressive strength. Most data values lie within ± 15% confidence lines, indicating a reasonably good prediction.

Table 6 Model summary for Eq. (1)

σ	R^2	Adjusted R^2	Predicted R^2
3.836	87.12%	86.66%	85.27%

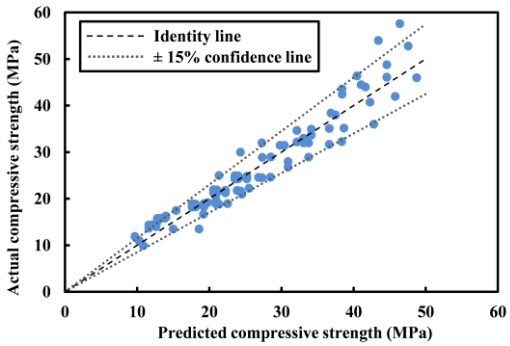

Fig. 13 Predicted compressive strength versus actual compressive strength

Subsequent to formulating Eq. (1), PAC mixes were produced to verify the equation. The maximum nominal size of sand used in this study was 2.36 mm and the smallest size of coarse aggregate in 10 mm coarse aggregates gradation was as small as 5 mm. As the minimum size of coarse aggregates is recommended to be at least four times the largest size of the fine aggregate used (Najjar *et al.* 2014, Orchard 1973), sand was excluded from the PAC mixes produced using 10 mm coarse aggregates to ensure efficient filling of voids by the grout in between the coarse aggregates. Table 7 shows the mix proportions along with the experimental and predicted compressive strength values of the PAC. The experimental compressive strength of the PAC specimens (PAC1 to PAC6) was close to the predicted compressive strength, implying a reliable prediction by Eq. (1).

4.2 Binder factor

The influence of GGBS and/or SF on the compressive strength of PAC at 28 days is indicated by the binder factor Beta ("β"). This value was derived from the experimental data. Table 4 shows β for the grout mixes obtained experimentally. β for the control grout mix (GRT-0000) was considered as a reference and was normalized to 1. β was calculated as the ratio between the compressive strength of the grout mix to the compressive strength of the control grout mix. β was analyzed statistically to derive a regression equation that fits the experimental data. Eq. (2)

Table 7 Mix proportion, experimental and predicted compressive strength of PAC

Mix ID	CA size (mm)	W/B	S/B	GGBS/B	SF/B	Experimental compressive strength (MPa)	Predicted compressive strength (MPa)	Percentage error (%)
PAC1	45	0.50	0.50	0.00	0.00	23.56	24.40	3.58
PAC2	10	0.40	0.00	0.00	0.00	41.77	37.97	9.10
PAC3	20	0.37	0.50	0.00	0.00	42.01	38.41	8.57
PAC4	20	0.37	0.00	0.00	0.00	34.90	37.23	6.69
PAC5	20	0.33	0.00	0.00	0.00	37.35	39.61	6.05
PAC6	10	0.33	0.00	0.00	0.00	44.90	42.12	6.19
PAC7	45	0.38	0.50	0.20	0.08	30.88	31.26	1.24
PAC8	20	0.55	0.30	0.35	0.00	21.95	22.96	4.60
PAC9	20	0.33	0.00	0.40	0.10	36.98	36.52	1.25
PAC10	20	0.45	0.20	0.15	0.02	33.34	31.40	5.81
PAC11	10	0.33	0.00	0.25	0.05	42.05	39.53	5.99
PAC12	10	0.35	0.00	0.00	0.10	48.33	45.11	6.66

Table 8 Model summary for Eq. (2)

σ	R^2	Adjusted R^2	Predicted R^2
0.019	95.55%	94.43%	89.30%

shows the empirical relationships between β, GGBS/B, and SF/B. Table 8 shows the model summary of Eq. (2). The R^2 and adjusted R^2 values are above 90%. Fig. 14 compares the predicted values against the experimental values of β. All data points lie well within ±10% confidence lines, indicating a reasonably good prediction.

$$\beta = 1 - 0.45\left(\frac{GGBS}{B}\right) + 1.02\left(\frac{SF}{B}\right) \quad (2)$$

Eq. (1) was modified to incorporate the influence of GGBS and/or SF by introducing β, as shown in Eq. (3).

$$f'_{c(GGBS,SF)} = (f'_c)(\beta \times \gamma) \text{ or } \gamma = \frac{f'_{c(GGBS,SF)}}{f'_c \, x \, \beta} \quad (3)$$

The correlation coefficient "γ" was introduced to correlate the compressive strength values of the grout and PAC incorporating GGBS and/or SF. PAC mixes with different grout mix proportions and coarse aggregate sizes were produced to determine γ. Table 9 shows the mix proportion and compressive strength outcomes of the PAC specimens. Efficient penetrability of grout through the coarse aggregate skeleton was ensured. Fig. 15 shows the γ value for the PAC mixes. According to Fig. 15, the correlation coefficient "γ" is close to 1. This indicates that with incorporation and/or variation in proportion of GGBS and SF, influence on compressive strength of grout and PAC is similar.

Hence, Eq. (4) predicts the 28-day compressive strength of PAC produced using GGBS and/or SF as a partial replacement of cement within the replacement ranges of 0 to 40% and 0 to 10%, respectively.

As γ=1, Eq. (3) was expressed as

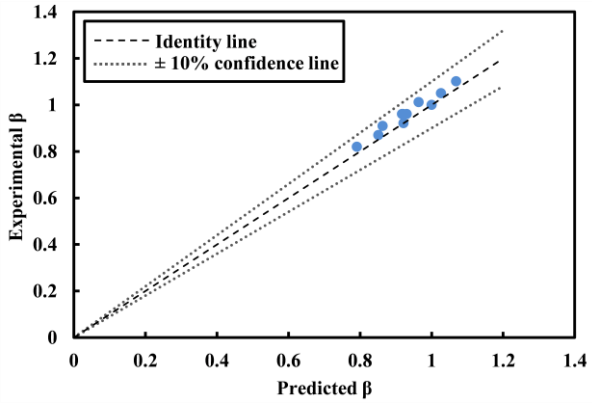

Fig. 14 Predicted β versus experimental β

$$f'_{c(GGBS,SF)} = (f'_c)(\beta) = \left\{64.23 - 5.03\left(\frac{CA}{20}\right) - 59.37\left(\frac{W}{B}\right) + 2.35\left(\frac{S}{B}\right)\right\}\left\{1 - 0.45\left(\frac{GGBS}{B}\right) + 1.02\left(\frac{SF}{B}\right)\right\} \quad (4)$$

PAC mixes were produced to verify the equation and are shown in Table 7. Data from literature used to obtain the above relation constitutes coarse aggregates of size as large as 63 mm, therefore, few mixes produced for verification were prepared using larger size coarse aggregates (45 mm). The results show that the compressive strength of PAC obtained experimentally was close to the predicted compressive strength. This indicates that Eq. (4) provides a reasonable prediction of the compressive strength of PAC at 28 days when it incorporates GGBS and/or SF. However, the relationship is limited to PAC with a GGBS/B ratio in the range of 0.00 to 0.40 and an SF/B ratio in the range of 0.00 to 0.10. The above relationship will assist in reducing the number of trials to attain the target strength while using supplementary cementitious materials. This will further help prevent the wastage of resources and impart environmental benefits to this unique method of producing concrete.

Table 9 Mix proportions and compressive strength of PAC for correlation coefficient γ

Mix no.	Coarse aggregate size (mm)	W/B	S/B	GGBS/B	SF/B	Compressive strength (MPa)
1	20	0.37	0.5	0	0	42.01
2	20	0.37	0.5	0.4	0	31.92
3	20	0.37	0.5	0	0.1	48.02
4	20	0.37	0.5	0.2	0.05	35.11
5	20	0.37	0.5	0.4	0.1	42.62
6	20	0.37	0	0	0	34.9
7	20	0.37	0	0.4	0	30.13
8	20	0.37	0	0	0.1	39.91
9	20	0.37	0	0.2	0.05	33.89
10	20	0.37	0	0.4	0.1	34.21
11	20	0.33	0	0	0	37.35
12	20	0.33	0	0.4	0	33.51
13	20	0.33	0	0	0.1	41.93
14	20	0.33	0	0.2	0.05	35.8
15	20	0.33	0	0.4	0.1	36.98
16	10	0.33	0	0	0	44.96
17	10	0.33	0	0.4	0	34.44
18	10	0.33	0	0	0.1	50.23
19	10	0.33	0	0.2	0.05	41.35
20	10	0.33	0	0.4	0.1	43.11

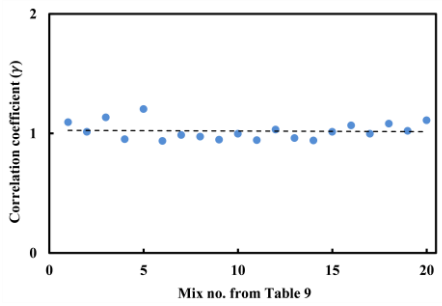

Fig. 15 Correlation coefficient γ

5. Conclusions

The present study investigates the effects of GGBS and SF on grout and PAC specimens. Grout proportions were optimized statistically using a factorial design. PAC was formed using different sizes of coarse aggregates. The flowability and compressive strength of grout were assessed. The mechanical properties of PAC were accessed in terms of compressive strength and splitting tensile strength. The durability of PAC was evaluated by chloride ion penetration tests and drying shrinkage tests. The main conclusions drawn from the study are as follows.

- GGBS increases the flowability and reduces the compressive strength of grout, whereas SF reduces the flowability and increases the compressive strength of grout. While SF has greater effects on the efflux time of grout than GGBS, indicating that a small increase or decrease in the SF content has a greater influence on the flowability of grout than GGBS, GGBS has a stronger effect on the compressive strength of grout than SF.
- SF improves both the compressive strength and splitting tensile strength of PAC, whereas GGBS decreases the compressive strength and splitting tensile strength of PAC. Both GGBS and SF improve the resistance to chloride ion penetration and increase the drying shrinkage of PAC.
- With a reduction in the coarse aggregate size from 20 mm to 10 mm, the compressive strength and splitting tensile strength of PAC increased. This was attributed to an increase in the bonding area between the coarse aggregates and grout and an increase in the mechanical interlocking between the coarse aggregates that improved the frictional properties.
- A reduction in the coarse aggregate size from 20 mm to 10 mm led to an increase in the resistance to chloride ion penetration. With the reduction in the coarse aggregate size, the void content of PAC was reduced. This reduced the amount of grout per surface area of the PAC, reducing the passages through which chloride ions could pass and subsequently improving the resistance to chloride ion penetration.
- The mix proportions along with the 28-day compressive strength values of PAC from the literature were analyzed statistically to derive empirical

relationships between the compressive strength of PAC and the CA, W/B, and S/B. The binder factor Beta was introduced to account for the variation in the compressive strength due to the incorporation of GGBS and/or SF. Eq. (4) predicts the 28-day compressive strength of PAC incorporating GGBS and/or SF at 0 to 40% and 0 to 10% by weight of the binder, respectively. The results predicted by the empirical relationship are in good agreement with those of mixes produced for verification.

Acknowledgements

This work was supported by the National Research Foundation of Korea (NRF) grant funded by the Korea government (MSIT) (No. 2021R1C1C1013864). The authors wish to express their gratitude for the financial support provided by The Hong Kong Polytechnic University. The authors are grateful for the technical support provided by the laboratories of the Department of Civil and Environmental Engineering, The Hong Kong Polytechnic University.

References

Abdelgader, H.S. (1995), "Polcrete economical method for dams", *MWA Int. Conf. Dam Eng.*, **1**, 1-4.

Abdelgader, H.S. (1996), "Effect of the quantity of sand on the compressive strength of two-stage concrete", *Mag. Concrete Res.*, **48**(4), 353-360. https://doi.org/10.1680/macr.1996.48.177.353.

Abdelgader, H.S. (1999), "How to design concrete produced by a two-stage concreting method", *Cement Concrete Res.*, **29**(3), 331-337. https://doi.org/10.1016/S0008-8846(98)00215-4.

Abdelgader, H.S. and Ben-Zeitun, A.E. (2005), "Tensile strength of two-stage concrete measured by double-punch and split tests", *Role of Concrete in Nuclear Facilities*, Thomas Telford Publishing, London, UK.

Abdelgader, H.S. and El-Baden, A.S. (2015), "Effect of silica fume on two-stage concrete strength", *IOP Conf. Ser.: Mater. Sci. Eng.*, **96**(1), 012043. https://doi.org/10.1088/1757-899X/96/1/012043.

Abdelgader, H.S., El-Baden, A.S., Abdurrahman, H.A. and Abdul Awal, A.S.M. (2018), "Two-stage concrete as a sustainable production", *MATEC Web Conf.*, **149**, 1-7. https://doi.org/10.1051/matecconf/201714902009.

Abdelgader, H.S. and Elgalhud, A.A. (2008), "Effect of grout proportions on strength of two-stage concrete", *Struct. Concrete*, **9**(3), 163-170. https://doi.org/10.1680/stco.2008.9.3.163.

Abdelgader, H.S. and Górski, J. (2002), "Influence of grout proportions on modulus of elasticity of two-stage concrete", *Mag. Concrete Res.*, **54**(4), 251-255. https://doi.org/10.1680/MACR.2002.54.4.251.

Abdelgader, H.S. and Górski, J. (2003), "Stress-strain relations and modulus of elasticity of two-stage concrete", *J. Mater. Civil Eng.*, **15**(4), 329-334. https://doi.org/10.1061/(asce)0899-1561(2003)15:4(329).

Abdelgader, H.S., Najjar, M. and Azabi, T.M. (2010), "Study of underwater concrete using two-stage (preplaced aggregate) concrete in Libya", *Struct. Concrete*, **11**(3), 161-165. https://doi.org/10.1680/stco.2010.11.3.161.

Abdelgader, H.S., Saud, A.F. and El-Baden, A.S. (2013), "Flexural strength of two-stage concrete", *Proceedings of the Third International Conference on Sustainable Construction Materials and Technologies (SCMT3)*, Kyoto, August.

ACI 211.1. (1996), Standard Practice for Selecting Proportions for Normal, Heavyweight, and Mass Concrete, American Concrete Institute, Farmington Hills, MI, USA.

ACI 233R. (1995), Ground Granulated Blast-Furnace Slag as a Cementitious Constituent in Concrete, American Concrete Institute, Farmington Hills, MI, USA.

ACI 304.1. (2005), Guide for the Use of Preplaced Aggregate Concrete for Structural and Mass Concrete Applications, American Concrete Institute, Farmington Hills, MI, USA.

ACI 363. (1997), State-of-the-Art Report on High-Strength Concrete, American Concrete Institute, Farmington Hills, MI, USA.

Alexander, K.M. and Wardlaw, J. (1960), "Dependence of cement-aggregate bond-strength on size of aggregate", *Nature*, **187**(4733), 230. https://doi.org/10.1038/187230a0.

ASTM C 1202. (2012), Standard Test Method for Electrical Indication of Concrete's Ability to Resist Chloride Ion Penetration, ASTM International, West Conshohocken, PA, USA.

ASTM C 150. (2017), Standard Specification for Portland Cement, ASTM International, West Conshohocken, PA, USA.

ASTM C 39. (2005), Standard Test Method for Compressive Strength of Cylindrical Concrete Specimens, ASTM International, West Conshohocken, PA, USA.

ASTM C 496. (2011), Standard Test Method for Splitting Tensile Strength of Cylindrical Concrete Specimens, ASTM International, West Conshohocken, PA, USA.

ASTM C 939. (2002), Standard Test Method for Flow of Grout for Preplaced Aggregate Concrete (Flow Cone Method), ASTM International, West Conshohocken, PA, USA.

ASTM C 940-R03. (2016), Standard Test Method for Expansion and Bleeding of Freshly Mixed Grout for Preplaced-Aggregate Concrete in the Laboratory, ASTM International, West Conshohocken, PA, USA.

ASTM C 942. (2008), Standard Test Method for Compressive Strength of Grouts for Preplaced-Aggregate Concrete in the Laboratory, ASTM International, West Conshohocken, PA, USA.

Awal Abdul, A.S. (1988), "Failure mechanism of prepacked concrete", *J. Struct. Eng.*, **3**(114), 727-732.

Bayer, R. (2004), *Use of Preplaced Aggregate Concrete for Mass Concrete Applications*, Middle East Technical University, Ankara, Türkiye.

Bisschop, J. and Van Mier, J.G.M. (2002), "How to study drying shrinkage microcracking in cement-based materials using optical and scanning electron microscopy?", *Cement Concrete Res.*, **32**(2), 279-287. https://doi.org/10.1016/S0008-8846(01)00671-8.

Bloem, D.L. and Gaynor, R.D. (1963), "Effects of aggregate properties on strength of concrete", *ACI J. Proc.*, **10(**60), 1429-1456.

BS EN 12504-1. (2009), Testing Concrete in Structures, Cored Specimens, Taking, Examining and Testing in Compression, British Standard Institution, London, UK.

BS EN 8500. (2002), Concrete Complementary-British Standard to BSEN206-1 Part 1: Method of Specifying and Guidance for the Specifier, Part 2: Specification for Constituent Materials and Concrete, British Standard Institution, London, UK.

BS ISO 1920-8. (2009), Determination of Drying Shrinkage of Concrete for Samples Prepared in the Field or in the Laboratory, British Standard Institution, London, UK.

Cheng, A., Huang, R., Wu, J. and Chen, C. (2005), "Influence of GGBS on durability and corrosion behavior of reinforced

concrete", *Mater. Chem. Phys.*, **93**, 404-411. https://doi.org/10.1016/j.matchemphys.2005.03.043.

Cheng, Y., Liu, S., Zhu, B., Liu, R. and Wang, Y. (2019), "Preparation of preplaced aggregate concrete and experimental study on its strength", *Constr. Build. Mater.*, **229**, 116847. https://doi.org/10.1016/j.conbuildmat.2019.116847.

Coo, M. and Pheeraphan, T. (2015), "Effect of sand, fly ash, and coarse aggregate gradation on preplaced aggregate concrete studied through factorial design", *Constr. Build. Mater.*, **93**, 812-821. https://doi.org/10.1016/j.conbuildmat.2015.05.086.

Coo, M. and Pheeraphan, T. (2016), "Effect of sand, fly ash and limestone powder on preplaced aggregate concrete mechanical properties and reinforced beam shear capacity", *Constr. Build. Mater.*, **120**, 581-592. https://doi.org/10.1016/j.conbuildmat.2016.05.128.

Cordon, W.A. and Gillespie, H.A. (1963), "Variables in concrete aggregates and Portland cement paste which influence the strength of concrete", *ACI J. Proc.*, **8**(60), 1029-1052.

Das, K.K. and Lam, E.S.S. (2019), "Feasibility of producing two-stage (preplaced aggregate) concrete by gravity process", *Struct. Concrete*, **21**(3), 1157-1163. https://doi.org/10.1002/suco.201900356.

Das, K.K., Lam, E.S.S. and Tang, H.H. (2020), "Partial replacement of cement by ground granulated blast furnace slag and silica fume in two-stage concrete (preplaced aggregate concrete)", *Struct. Concrete*, **22**(S1), E466-E473. https://doi.org/10.1002/suco.201900494.

Davis, R.E. (1960), "Prepakt method of concrete repair", *ACI Mater. J.*, **8**(57), 155-172. https://doi.org/DOI: 10.14359/8016.

Diamond, S. and Sahu, S. (2006), "Densified silica fume: Particle sizes and dispersion in concrete", *Mater. Struct. Mater. Constr.*, **39**(9), 849-859. https://doi.org/10.1617/s11527-006-9087-y.

Emmons, P. (1992), *Concrete Repair and Maintenance Illustrated: Problem Analysis, Repair Strategy, Techniques*, John Wiley & Sons, Hoboken, NJ, USA.

Fu, T., Deboodt, T. and Ideker, J.H. (2016), "Development of shrinkage limit specification for high performance concrete used in bridge decks", *Cement Concrete Compos.*, **72**, 17-26. https://doi.org/10.1016/j.cemconcomp.2016.05.015.

Guo, Y., Wu, J., Wang, C. and Zhang, F. (2020), "Study on the influence of the shape and size of coarse aggregate on the strength of concrete", *IOP Conf. Ser.: Mater. Sci. Eng.*, **780**(4), https://doi.org/10.1088/1757-899X/780/4/042008.

IS 10262. (2009), Guidelines for Concrete Mix Design Proportioning, Bureau of Indian Standards, New Delhi, India.

Johari, M., Brooks, J. and Kabir, S. (2011), "Influence of supplementary cementitious materials on engineering properties of high strength concrete", *Constr. Build. Mater.*, **25**, 2639-2648. https://doi.org/10.1016/j.conbuildmat.2010.12.013.

Khan, M.I. and Siddique, R. (2011), "Utilization of silica fume in concrete: Review of durability properties", *Resour. Conserv. Recyc.*, **57**, 30-35. https://doi.org/10.1016/j.resconrec.2011.09.016.

Khatib, J.M. and Hibbert, J.J. (2005), "Selected engineering properties of concrete incorporating slag and metakaolin", *Constr. Build. Mater.*, **19**(6), 460-472. https://doi.org/10.1016/j.conbuildmat.2004.07.017.

Krakowiak, K.J., Thomas, J.J., James, S., Abuhaikal, M. and Ulm, F.J. (2018), "Development of silica-enriched cement-based materials with improved aging resistance for application in high-temperature environments", *Cement Concrete Res.*, **105**, 91-110. https://doi.org/10.1016/j.cemconres.2018.01.004.

Lv, J., Zhou, T., Du, Q., Li, K. and Jin, L. (2020), "Research on the bond behavior of preplaced", *Mater.*, **2**(13), 300.

Mohammadhosseini, H., Abdul Awal, A.S.M. and Sam, A.R.M. (2016), "Mechanical and thermal properties of prepacked aggregate concrete incorporating palm oil fuel ash", *Sadhana Acad. Proc. Eng. Sci.*, **41**(10), 1235-1244. https://doi.org/10.1007/s12046-016-0549-9.

Mohammadhosseini, H., Tahir, M.M., Alaskar, A., Alabduljabbar, H. and Alyousef, R. (2020), "Enhancement of strength and transport properties of a novel preplaced aggregate fiber reinforced concrete by adding waste polypropylene carpet fibers", *J. Build. Eng.*, **27**, 101003. https://doi.org/10.1016/j.jobe.2019.101003.

Montgomery, D.C. (2017), *Design and Analysis of Experiments*, John Wiley & Sons, Hoboken, NJ, USA.

Najjar, M. (2016), "Innovating two-stage concrete with improved rheological, mechanical and durability properties", Doctoral dissertation, The University of Western Ontario, Ontario, Canada.

Najjar, M.F., Soliman, A.M. and Nehdi, M.L. (2014), "Critical overview of two-stage concrete: Properties and applications", *Constr. Build. Mater.*, **62**, 47-58. https://doi.org/10.1016/j.conbuildmat.2014.03.021.

Najjar, M.F., Soliman, A.M. and Nehdi, M.L. (2016), "Two-stage concrete made with single, binary and ternary binders", *Mater. Struct. Mater. Constr.*, **49**(1-2), 317-327. https://doi.org/10.1617/s11527-014-0499-9.

Nehdi, M.L., Najjar, M.F., Soliman, A.M. and Azabi, T.M. (2017a), "Novel steel fibre-reinforced preplaced aggregate concrete with superior mechanical performance", *Cement Concrete Compos.*, **82**, 242-251. https://doi.org/10.1016/j.cemconcomp.2017.07.002.

Nehdi, M.L., Najjar, M.F., Soliman, A.M. and Azabi, T.M. (2017b), "Novel steel fibre-reinforced preplaced aggregate concrete with superior mechanical performance. *Cement Concrete Compos.*, **82**, 242-251. https://doi.org/10.1016/j.cemconcomp.2017.07.002.

Neville, A.M. (2011), *Properties of Concrete*, London Pearson Education Limited, London, UK.

Nochaiya, T., Wongkeo, W. and Chaipanich, A. (2010), "Utilization of fly ash with silica fume and properties of Portland cement-fly ash-silica fume concrete", *Fuel*, **89**(3), 768-774. https://doi.org/10.1016/j.fuel.2009.10.003.

Nowek, A., Kaszubski, P., Abdelgader, H.S. and Górski, J. (2007), "Effect of admixtures on fresh grout and two-stage (pre-placed aggregate) concrete", *Struct. Concrete*, **8**(1), 17-23. https://doi.org/10.1680/stco.2007.8.1.17.

O'Malley, J. and Abdelgader, H.S. (2010), "Investigation into viability of using two-stage (pre-placed aggregate) concrete in Irish setting", *Front. Arch. Civil Eng. Chin.*, **4**(1), 127-132. https://doi.org/10.1007/s11709-010-0007-4.

Oner, A. and Akyuz, S. (2007), "An experimental study on optimum usage of GGBS for the compressive strength of concrete", *Cement Concrete Compos.*, **29**(6), 505-514. https://doi.org/10.1016/j.cemconcomp.2007.01.001.

Orchard, D.F. (1973), *Concrete Technology*, 3rd Edition, Applied Science Publishers Ltd., London, UK.

Poon, C.S., Kou, S.C. and Lam, L. (2006), "Compressive strength, chloride diffusivity and pore structure of high performance metakaolin and silica fume concrete", *Constr. Build. Mater.*, **20**(10), 858-865. https://doi.org/10.1016/j.conbuildmat.2005.07.001.

Prasad, N. and Murali, G. (2021), "Exploring the impact performance of functionally-graded preplaced aggregate concrete incorporating steel and polypropylene fibres", *J. Build. Eng.*, **35**, 102077. https://doi.org/10.1016/j.jobe.2020.102077.

Rajabi, A.M. and Omidi Moaf, F. (2017), "Simple empirical formula to estimate the main geomechanical parameters of preplaced aggregate concrete and conventional concrete", *Constr. Build. Mater.*, **146**, 485-492. https://doi.org/10.1016/j.conbuildmat.2017.04.089.

Rajabi, A.M., Omidi Moaf, F. and Abdelgader, H.S. (2020),

"Evaluation of mechanical properties of two-stage concrete and conventional concrete using nondestructive tests", *J. Mater. Civil Eng.*, **32**(7), 04020185. https://doi.org/10.1061/(asce)mt.1943-5533.0003247.

Rao, G.A. (2001), "Long-term drying shrinkage of mortar - influence of silica fume and size of fine aggregate", *Cement Concrete Res.*, **31**, 171-175. https://doi.org/10.1016/S0008-8846(00)00347-1.

Rashid, M.A. and Mansur, M.A. (2009), "Considerations in producing high strength concrete", *J. Civil Eng.*, **37**(1), 53-63.

Saluja, S., Kaur, K., Goyal, S. and Bhattacharjee, B. (2019), "Assessing the effect of GGBS content and aggregate characteristics on drying shrinkage of roller compacted concrete", *Constr. Build. Mater.*, **201**, 72-80. https://doi.org/10.1016/j.conbuildmat.2018.12.179.

Saud, A.F., Abdelgader, H.S. and El-Baden, A.S. (2014), "Compressive and tensile strength of two-stage concrete", *Adv. Mater. Res.*, **893**, 585-592. https://doi.org/10.4028/www.scientific.net/AMR.893.585.

Siddique, S., Kim, H., Son, H. and Jang, J.G. (2021), "Characteristics of preplaced aggregate concrete fabricated with alkali-activated slag/fly ash cements", *Mater.*, **14**(3), 1-17. https://doi.org/10.3390/ma14030591.

St. John, D. (1994), *The Dispersion of Silica Fume*, Industrial Research Limited, Wellington, NZ.

Stempkowska, A., Gawenda, T., Naziemiec, Z., Ostrowski, K.A., Saramak, D. and Surowiak, A. (2020), "Impact of the geometrical parameters of dolomite coarse aggregate on the thermal and mechanic properties of preplaced aggregate concrete", *Mater.*, **13**(19), 1-16. https://doi.org/10.3390/ma13194358.

Tumidajski, P.J. and Gong, B. (2006), "Effect of coarse aggregate size on strength and workability of concrete", *Can. J. Civil Eng.*, **2**(33), 206-213. https://doi.org/10.1139/l05-090.

Tuyan, M., Zhang, L.V. and Nehdi, M.L. (2020a), "Development of sustainable preplaced aggregate concrete with alkali-activated slag grout", *Constr. Build. Mater.*, **263**, 120227. https://doi.org/10.1016/j.conbuildmat.2020.120227.

Tuyan, M., Zhang, L.V. and Nehdi, M.L. (2020b), "Development of sustainable alkali-activated slag grout for preplaced aggregate concrete", *J. Clean. Prod.*, **277**, 123488. https://doi.org/10.1016/j.jclepro.2020.123488.

Varghese, L., Kanta Rao, V. and Parameswaran, L. (2017), "Effect of nanosilica on drying shrinkage and creep properties of cement concrete", *Adv. Mater. Proc.*, **2**(1), 56-60. https://doi.org/10.5185/amp.2017/113.

Vieira, M., Bettencourt, A., Camelo, A. and Ferreira, J. (2010), "Self-compacting mortar for mass concrete application with PAC technology", *Proceedings of SCC2010*, Montreal, Canada, September.

Yildirim, H., Ilica, T. and Sengul, O. (2011), "Effect of cement type on the resistance of concrete against chloride penetration", *Constr. Build. Mater.*, **25**(3), 1282-1288. https://doi.org/10.1016/j.conbuildmat.2010.09.023.

CC